Multiple scattering effects in depth resolution of elastic recoil detection [1]

Leszek S. Wielunski*, Edit Szilágyi** and Geoffrey L. Harding*
* CSIRO, Telecommunications and Industrial Physics, PO Box 218, Lindfield, NSW 2070, Australia
**KFKI Research Institute for Particle and Nuclear Physics,
P.O. Box 49, H-1525 Budapest, Hungary

Introduction: Elastic Recoil Detection (ERD) is used to profile hydrogen and other low mass elements in thin films at surface and interfaces [1-3] in a similar way that Rutherford Backscattering Spectroscopy (RBS) is used to detect and profile heavy elements. It is often assumed that the depth resolutions of these two techniques are similar. However, in contrast to typical RBS, the depth resolution of ERD is limited substantially by multiple scattering [4]. In experimental data analysis and/or spectra simulations of a typical RBS measurement multiple scattering effects are often ignored. Computer programs used in IBA, such as RUMP, HYPRA or RBX do not include multiple scattering effects at all [5-7].

In this paper, using practical thin metal structures with films containing intentionally introduced hydrogen, we demonstrate experimental ERD depth resolution and sensitivity limitations. The effects of sample material and scattering angle are also discussed.

Multiple scattering effects: There are two effects arising from the statistical nature of the energy loss process in material to be considered: the spread in ion energy and that in the ion direction. The direct energy spread, called energy straggling, is often small and it is well described in the literature [8,9]. In the case of typical RBS the energy straggling is the main process responsible for the reduction of depth resolution, however in the case of ERD the depth resolution is strongly affected by the spread in ion direction due to the angular sensitivity of ERD kinematics.

The spread in ion direction is always accompanied by a lateral displacement from the average path. In this way, multiple scattering results in a spread of the detected ion energy by two basically different mechanisms: i) the angular spread directly changes the scattering /recoil angle and through the kinematics of the process it also changes the energy of the detected ions (angular spread). ii) The lateral displacement transforms into a path length variation, which through the corresponding stopping power causes another energy spread contribution (lateral spread).

For RBS analysis with a scattering angle of ~ 180° the energy of the scattered ion depends only slightly on the scattering angle and the final depth resolution changes slightly as a result of the angular spread [10].

In ERD measurement, in contrast to RBS, as a consequence of the scattering kinematics and the geometry of ERD, multiple scattering effects are rather large. The energy of the recoiled atom, E, strongly depends on the recoil angle, $\varnothing$: $E = 4E_0M_1M_2(M_1+M_2)^{-2}\cos^2\varnothing$, where E_0 is the ion energy before the reaction event and M_1, and M_2 are the ion and recoil mass, respectively [11]. For nominal recoil angles typical in ERD of $\varnothing_{nom} = 20° - 30°$, the detected ion energy will be strongly affected by changes in the incident and/or recoil ion direction $\Delta\Phi$ (as the recoil angle is $\varnothing_{nom} = \varnothing+\Delta\Phi$). Additionally, because of the glancing incidence and outgoing angles in reflection ERD geometries (both of them are usually less than 15°), the lateral spread for both the inward and outward path is also significant.

The FWHM of the angular distribution caused by multiple scattering was estimated using the method of Sigmund and Winterbon [12,13] and the effective ERD energy and depth resolutions were compared with experimental results [4]. It was shown that this multiple scattering effect is dominant and limits substantially the depth resolution of ERD analysis in all cases, except for surface contamination. This effect is stronger in high Z materials as a consequence of larger scattering angles and cross-sections in multiple scattering [4,14].

One of us has developed a computer program, DEPTH, which calculates the energy (depth) resolution of RBS, ERD and other IBA methods taking into account all the important effects including multiple scattering [15]. The program now has been developed further. It calculates the energy and depth resolution for multilayers, and it is also possible to construct and save the simulated energy spectra of ERD [16]. In the simulation the cross section for the $He^4(H^1,He^4)H^1$ reaction is obtained by fitting Benenson's data [17].

[1] The work was partially supported by Hungarian OTKA grant No. F019165.

In this work the new version of DEPTH was used to calculate the energy resolution of ERD in various metals (Al, Cr, Zr and W) and for a number of different depths. The results are compared to a simple ERD simulation using the RBX program without taking into account multiple scattering. In this case only the geometrical spread and the energy straggling in the sample and absorber foil were considered [7].

Experimental: Four different metals: Al, Cr, W and Zr have been used to produce four special samples for ERD depth resolution study. Each sample contains three layers of the same metal deposited by magnetron sputtering onto typical semiconductor quality silicon wafer. The middle layer contains hydrocarbons introduced during deposition [18]. The thicknesses of the different metal films were chosen to be almost equivalent to each other in ion energy loss for the 2 MeV ^{4}He ions used in RBS, i.e., Al - 370 nm, Cr - 135 nm, Zr - 200 nm and W - 110 nm. The layer structure of each sample was analysed using 2 MeV ^{4}He RBS. The RBS results are shown on the bottom parts of Figs 1 – 4. ERD spectra of the same samples taken at 20° and 32° recoil angles are shown in the same figures.

The RBS and ERD analysis were performed in the same vacuum chamber at a pressure level of about 0.05 mPa. For RBS analysis the samples were first positioned normal to a 2 MeV ^{4}He beam from a tandem accelerator and the scattered ^{4}He ions were detected by a standard silicon surface barrier detector positioned at a scattering angle of 160°.

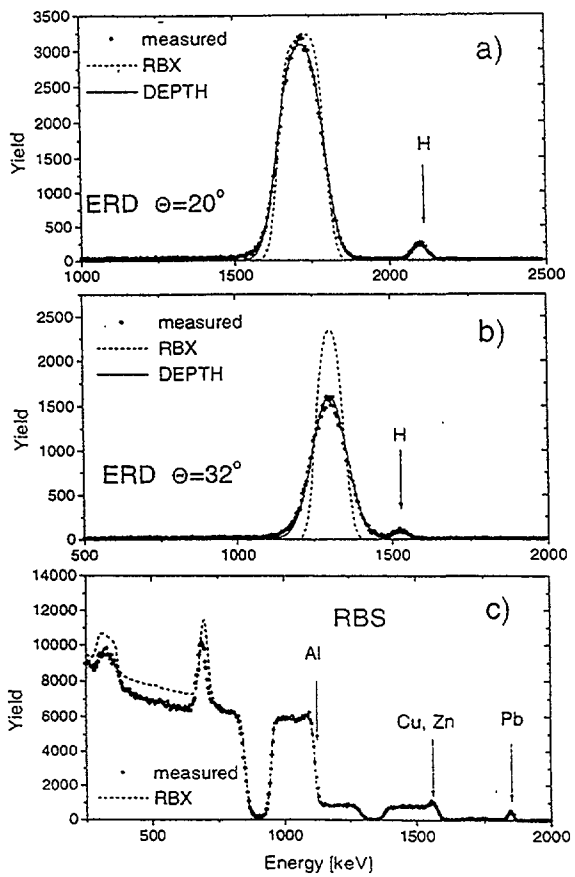

Fig. 1. Experimental 4.5 MeV ^{4}He ERD spectra in a 20° and 32° scattering geometry (a and b) from the Al sample compared to RBX and DEPTH simulations. The sample structure determined from the 2 MeV ^{4}He RBS analysis and RBX simulation shown in part (c); is 370 nm of $Al_{0.975}Cu_{0.015}Zn_{0.01}$ with very small amounts of Pb, Zn and Cu on the surface. The second layer is a thick Hydrocarbon (CH) layer with a negligible metal content and the third layer is about the same composition and thickness as the first one. The substrate was silicon.

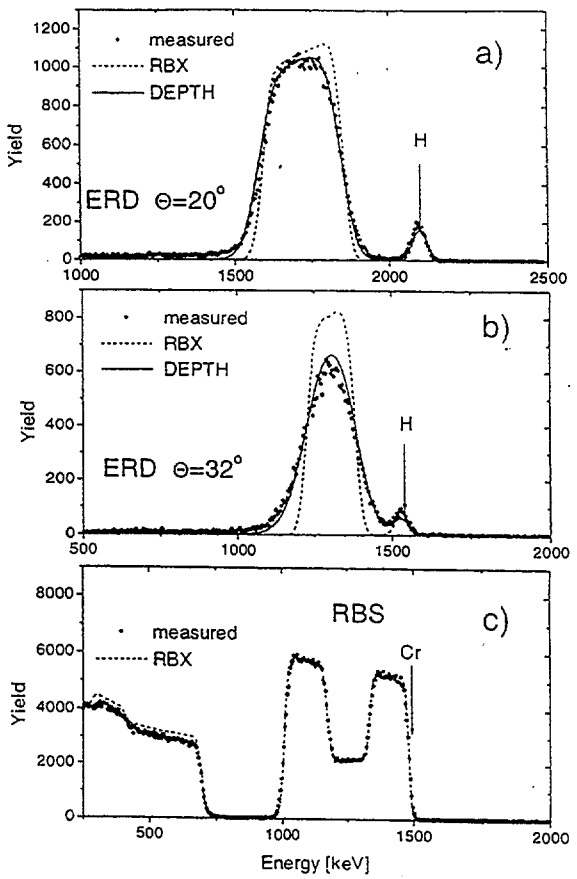

Fig. 2. Experimental 4.5 MeV ^{4}He ERD spectra in a 20° and 32° scattering geometry (a and b) from the Cr sample compared to RBX and DEPTH simulations. The sample structure determined from 2 MeV ^{4}He RBS analysis and RBX simulation shown in part (c); is 135 nm of Cr on uniform Cr hydrogenated layer ($Cr_{0.18}C_{0.64}H_{0.18}$) on 135 nm of Cr on Si.

In order to perform ERD analysis, the ion energy was increased to 4.5 MeV and the samples were rotated to 75° and 80° from the normal position. The recoiled H atoms were detected by a second surface barrier detector positioned alternatively at recoil angle of 32° or 20°. A 24 μm thick mylar absorber foil was mounted in front of this detector to absorb the scattered ^{4}He ions. Using a standard ion beam analysis system HYPRA [6] the RBS and ERD spectra were recorded into 512 channels with an energy conversion of about 4.37 keV/channel in RBS and 4.6 keV/channel in ERD.

Results: Figs 1c, – 4c show the RBS spectra of all samples used in this work. The layer structures obtained by RBX simulation of the above spectra are indicated in figure captions. In general, all samples contain a uniform hydrocarbonated metal layer between two reasonably pure metal films.

Two ERD spectra from the Al sample are shown in Figs 1a and 1b. In the same figures, the ERD spectra which were simulated by RBX using the same composition profile as used in RBS simulation for Fig. 1c are also shown (dashed line). Note, that RBX simulations do not include multiple scattering. The solid lines show simulated ERD spectra by DEPTH as described above. The agreement between experimental data and DEPTH simulations is excellent. The difference between these two simulations (RBX and DEPTH) is a measure of multiple scattering effects in this ERD measurement. It is clear, that the depth resolution is better in the 20° scattering geometry.

DEPTH simulations for the Cr sample in Figs 2a and 2b agree very well again with the experimental ERD data. As for Al, the real energy resolution is again strongly limited by multiple scattering (cf. RBX simulations) and it is better again at 20° recoil angle.

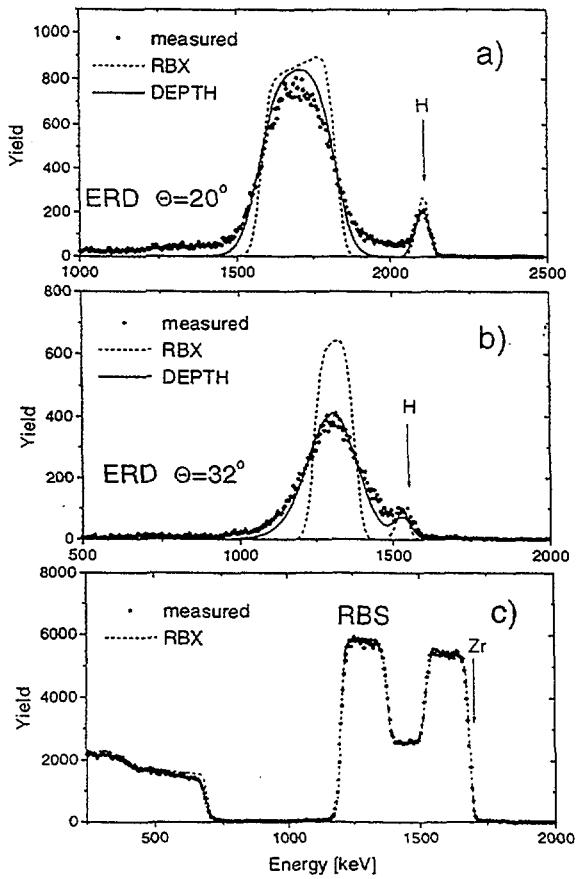

Fig. 3. Experimental 4.5 MeV ^{4}He ERD spectra in a 20° and 32° scattering geometry (a and b) from the Zr sample compared to RBX and DEPTH simulations. The sample structure determined from 2 MeV ^{4}He RBS analysis and RBX simulation shown in part (c); is 200 nm of Zr on Zr hydrogenated layer ($Zr_{0.18}C_{0.66}H_{0.16}$) on 200 nm of Zr on Si.

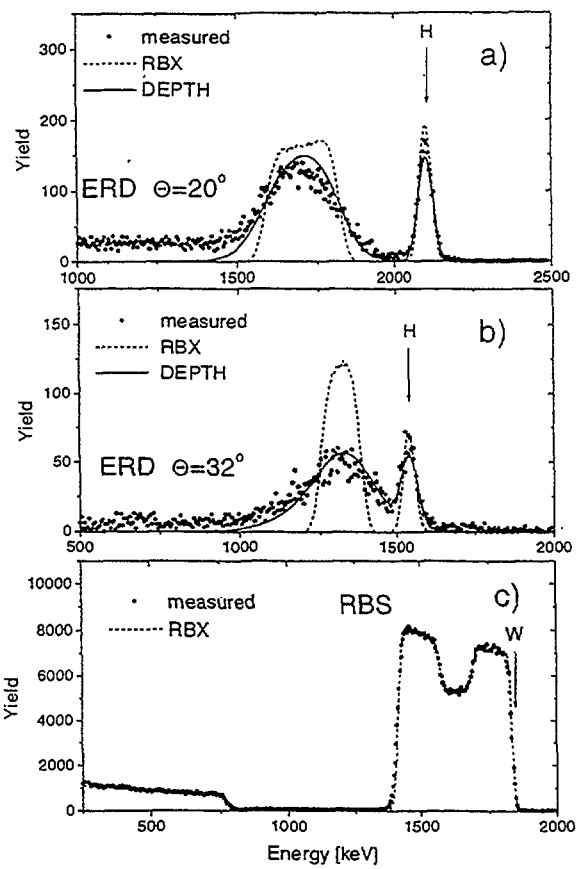

Fig. 4. Experimental 4.5 MeV ^{4}He ERD spectra in a 20° and 32° scattering geometry (a and b) from the W sample compared to RBX and DEPTH simulations. The sample structure determined from 2 MeV ^{4}He RBS analysis and RBX simulation shown in part (c); is 110 nm of W (most likely containing 26 at% of C) on uniform W-hydrogenated layer ($W_{0.32}C_{0.63}H_{0.05}$) on a further 110 nm of W (most likely containing 23 at% of C) on Si.

For the Zr sample, the DEPTH simulation agrees in general with the experimental data in Figs 3a and 3b, however, in the case of 20° scattering angle the tails in the low energy region of the experimental data (1000 keV-1500 keV) and also at high energy (about 2000 keV) are not predicted either by DEPTH or RBX. These types of tails were observed previously in ERD experiments and have been explained by double scattering in the sample material [4].

For the W sample, the DEPTH simulations of ERD spectra in Figs 4a and 4b are in good agreement with experimental data except for the low energy tails that are even larger now. The sensitivity and the energy resolution is even more reduced in this case.

Discussion: The width of the H surface peak is about 60 keV (FWHM) and it is a measure of the energy resolution of the ERD detection system also including the energy spread related to the detector solid angle and the energy straggling in the absorber foil. The H signal from the hydrogenated metal shows a substantially reduced depth resolution. This depth resolution is well predicted by DEPTH in all the studied metals and it is comparable to the individual film thickness used in this work.

In all figures ERD spectra and their simulations, using RBX code, show better agreement for 20° than for 32° scattering angle. This observation can be explained by the very strong kinematic angular energy dependence: $E \sim \cos^2\varnothing$, regardless of the fact that the average multiple scattering angle is of course higher for 20° than for 32° (due to longer ion path in the sample material).

Conclusions: Multiple scattering is the major process responsible for this deterioration of the energy resolution in ERD. Reducing the scattering angle helps to improve the ERD depth resolution, but at the same time, due to an increased double scattering background the sensitivity unfortunately decreases. The ERD depth resolution is reduced also by increasing the depth and/or the atomic number of sample material.

The results presented in this work agree well with the theoretically predicted multiple scattering effects and clearly indicate that the reduced depth resolution of ERD limits its applications, especially in the practical case of multilayer structures. It must be pointed out that this effect is related to the nature of the small angle scattering in a reflection geometry and it can be reduced only in transmission ERD (0° recoils). Unfortunately, in most applications samples cannot be studied in transmission geometry [19].

References:

[1] L.S. Wielunski, R.E. Benenson and W.A. Lanford, Nucl. Instr. and Meth. 218 (1983) 120.
[2] A. Turos and O. Meyer, Nucl. Instr. and Meth. B 4 (1984) 92.
[3] J. E.E. Baglin, A.J. Kellock, V.R. Deline, M.A. Crockett and A.H. Shih, Nucl. Instr. and Meth. B 64 (1992) 496.
[4] L.S. Wielunski, Nuclear Instr. and Meth. B118 (1996) 256.
[5] L.R. Doolittle, Nucl. Instr. and Meth. 92 (1971) 481.
[6] HYPRA RBS data collection and analysis program, Charles Evans and Associates, Redwood City, California, USA.
[7] E. Kótai, Nucl. Instr. and Meth. B 85 (1996) 588.
[8] W.K. Chu, Phys. Rev. 13 (1976) 2057.
[9] Q. Yang, D.J. O'Connor and Zhonglie Wang, Nucl. Instr. and Meth. B61 (1991) 149.
[10] J.A. Leavitt, L. C. McIntyre and M.R. Weller in Handbook of Modern Ion Beam Materials Analysis, eds. J.R. Tesmer and M. Nastasi (Materials Research Society, 1995) p. 39.
[11] J. C. Barbour and B.L. Doyle in Handbook of Modern Ion Beam Materials Analysis, eds. J.R. Tesmer and M. Nastasi (Materials Research Society, 1995) p. 90.
[12] J.R. Bird, R.A. Brown, D.D. Cohen and J.S. Williams in Ion Beams for Materials Analysis, eds. J.R. Bird and J. S. Williams (Academic Press 1989) p. 620.
[13] P. Sigmund and K.B. Winterbon, Nucl. Instr. and Meth. 119 (1974) 541.
[14] L.S. Wielunski, Mat. Sci. Forum 248-249 (1997) 369.
[15] E. Szilágyi, F. Pászti and G. Amsel, Nucl. Instr. and Meth. B 100 (1995) 103.
[16] E. Szilágyi, L. S. Wielunski, F. Pászti, IBA-13 Intern. Confer. to be published in NIM-B (1998).
[17] R.E. Benenson, L.S. Wielunski and W.A, Lanford, Nucl. Instr. and Meth. B 15 (1986) 453.
[18] S. Craig and G.L. Harding, Thin Solid Films 97 (1982) 345.
[19] L.Wielunski, R.E. Benenson, K. Horn and W.A. Lanford, Nucl. Instr. and Meth. B15 (1986) 469.